

Immunologic and Tissue Biocompatibility of Flexible/Stretchable Electronics and Optoelectronics

Gayoung Park, Hyun-Joong Chung, Kwanghee Kim, Seon Ah Lim, Jiyoung Kim, Yun-Soung Kim, Yuhao Liu, Woon-Hong Yeo, Rak-Hwan Kim, Stanley S. Kim, Jong-Seon Kim, Yei Hwan Jung, Tae-il Kim, Cassian Yee, John A. Rogers,* and Kyung-Mi Lee*

Recent development of flexible/stretchable integrated electronic sensors and stimulation systems has the potential to establish an important paradigm for implantable electronic devices, where shapes and mechanical properties are matched to those of biological tissues and organs. Demonstrations of tissue and immune biocompatibility are fundamental requirements for application of such kinds of electronics for long-term use in the body. Here, a comprehensive set of experiments studies biocompatibility on four representative flexible/stretchable device platforms, selected on the basis of their versatility and relevance in clinical usage. The devices include flexible silicon field effect transistors (FETs) on polyimide and stretchable silicon FETs, InGaN light-emitting diodes (LEDs), and AlInGaP LEDs, each on low modulus silicone substrates. Direct cytotoxicity measured by exposure of a surrogate fibroblast line and leachable toxicity by minimum essential medium extraction testing reveal that all of these devices are non-cytotoxic. In vivo immunologic and tissue biocompatibility testing in mice indicate no local inflammation or systemic immunologic responses after four weeks of subcutaneous implantation. The results show that these new classes of flexible implantable devices are suitable for introduction into clinical studies as long-term implantable electronics.

1. Introduction

Many classes of implantable electronic devices are currently in widespread use, with examples that range from pacemakers to cochlear implants and deep brain stimulators.^[1–3]

G. Park, Dr. K. Kim, S. A. Lim, J. Kim, Prof. K.-M. Lee
Global Research Laboratory
Department of Biochemistry and Molecular Biology
Korea University College of Medicine
Seoul, 136–713, Republic of Korea
E-mail: kyunglee@korea.ac.kr
Dr. H.-J. Chung, Y.-S. Kim, Y. Liu, Dr. W.-H. Yeo, Dr. R.-H. Kim, S. S. Kim,
J.-S. Kim, Y. H. Jung, Dr. T.-i. Kim, Prof. J. A. Rogers
Department of Materials Science and Engineering, Chemistry,
Mechanical Science and Engineering, Electrical and Computer Engineering
Beckman Institute for Advanced Science and Technology, and Frederick
Seitz Materials Research Laboratory
University of Illinois at Urbana-Champaign
Urbana, IL, 61801, USA
E-mail: jrogers@illinois.edu

DOI: 10.1002/adhm.201300220

In all cases, the electronics exist in sealed and rigid containers, with interfaces to the tissue that are restricted to one or several point contact electrodes. New classes of flexible/stretchable integrated electronic sensor and stimulation systems^[4–16] possess an exceptional ability to conform to organ topography,^[17–21] with significant potential for health/function monitoring and therapeutic intervention.^[4,6,18–22] Such systems include heterogeneous collections of hard electronic materials (e.g., semiconductor-grade silicon) and soft substrates (e.g., silicone rubber) that adhere to body surfaces via van der Waals and capillary interactions, with low modulus, elastic responses to large strain deformations. Unlike conventional hard electronics, the soft, “tissue-like” mechanics of these newer devices enable them to accommodate the natural movements and surface irregularities of vital organs, thereby reducing the probability of inflammation and permanent damage to the tissue by mechanical motion.^[23] Con-

formal sensors for high-resolution electrocorticography,^[6] multifunctional “epidermal” electronics for biopotential measurement,^[18] and monitoring sheets for mapping cardiac electrophysiology^[4,22] have been demonstrated. Although initial work focused primarily on temporary monitoring and

Prof. H.-J. Chung
Department of Chemical and Materials Engineering
University of Alberta
Edmonton, AB, T6G 2V4, Canada
Prof. T.-i. Kim
School of Chemical Engineering
Sungkyunkwan University (SKKU)
Suwon, 440–746, Korea

Dr. C. Yee
Department of Melanoma Medical Oncology and Immunology
U.T. MD Anderson Cancer Center, Houston, TX, 77030, USA



therapeutic applications, future opportunities include long-term implantation with active biotic/abiotic interfaces,^[24] with integration of stretchable batteries^[25] and wireless power and communication systems.^[26]

To design electronic devices capable of long-term implantation, issues in tissue and immunologic biocompatibility must be addressed. Tissue biocompatibility refers to the local non-toxic, non-thrombogenic, non-carcinogenic, and non-mutagenic properties of implantable devices^[27] while immunologic biocompatibility refers more specifically to the acute inflammatory and chronic immune responses elicited by a foreign body at both local and systemic levels. In this study, we selected four prototypic flexible/stretchable devices as potential candidates for development into long-term implantable flexible electronics. These devices, chosen on the basis of their versatility and relevance to clinical usage, include flexible silicon field effect transistors (FETs) on polyimide, stretchable silicon FETs, InGaN light-emitting diodes (LEDs), and AlInGaPAs LEDs, on low modulus silicone platforms.

We performed comprehensive biocompatibility analysis using both in vitro direct and indirect leachable cytotoxicity assays by exposing the devices and constituent materials to a surrogate fibroblast line. Long-term in vivo immunologic and tissue biocompatibility analyses were performed in mice at four weeks following subcutaneous implantation of each flexible/stretchable device. Local inflammatory and systemic immunologic responses were assessed by histology, cytokine analysis, and immune cell profiling. To our knowledge, these studies represent the first comprehensive assessments of tissue and immunologic biocompatibility of integrated flexible/stretchable electronic and optoelectronic sub-systems that contain FETs, LEDs, and metallic interconnects, embedded in insulating substrates. These data establish a biocompatibility profile for prospectively evaluating an emerging class of implantable devices, with potential for long-term use in humans.

2. Results

2.1. Direct Cytotoxicity Tests

Semiconductor components and associated interconnects provide active functionality in electronics/optoelectronics. The studied devices incorporate diverse materials, including both organics and inorganics, certain of which possess some level of toxicity. The biocompatibility is determined not only by toxicity of individual components, but by their configuration in these devices and their associated fabrication processes.^[28] In addition, depending on required operation, certain materials are designed to be in direct contact with the surrounding bio-system; others remain encapsulated and unexposed. As a result, the overall design, device architecture, and fabrication procedures can be as important in establishing biocompatibility as the selection of materials themselves.^[29]

Four types of flexible/stretchable devices (Si FETs on silicone, Si FETs on polyimide, InGaN LEDs on silicone, and AlInGaPAs LEDs on silicone) were fabricated for in vitro cytotoxicity tests (**Figure 1**). Implantation involves direct contact with surrounding tissues and is followed by infiltration of immune cells responding to a foreign body. As a result, cytotoxicity may be observed not only on neighboring stromal cells but also on the infiltrating immune cells. The effects of short-term cytotoxicity on cells predicted to encounter the implanted device are, therefore, of interest. L929 mouse fibroblast cell lines and whole splenocytes harvested from mouse spleen served as surrogates for the cells in contact with the implanted devices. Evaluations included direct contact assays as well as extraction tests to assess the cytotoxicity of leachable agents. FDA-approved high-density polyethylene (HDPE),^[30] which is known to be safe and nontoxic, and polyurethane containing 0.1% zinc diethyldithiocarbamate (PU-ZDEC),^[31] which causes cytotoxicity and cell death, served as negative and positive controls, respectively, in all experiments.

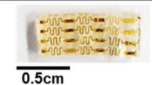



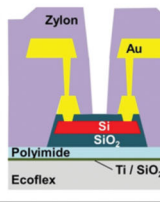
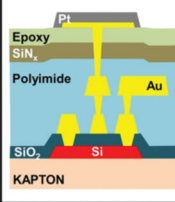
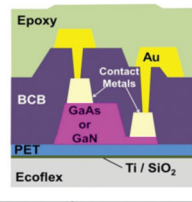
		Silicon FET on Ecoflex	Silicon FET on Kapton	InGaN LED on Ecoflex	AlInGaPAs LED on Ecoflex
Device					
Architecture					
Material	Semiconductor	Silicon (single crystal)	Silicon (single crystal)	InGaN (Molecular beam epitaxy)	AlInGaPAs (Molecular beam epitaxy)
	Interconnect & Electrode	Cr, Au	Cr, Au, Pt	Cr, Au, In, Ni, Ti	Cr, Au, Pd, Pt, Ge
	Insulator & Passivation	<ul style="list-style-type: none"> ▪ SiO₂ ▪ Polyimide ▪ Zylon 	<ul style="list-style-type: none"> ▪ SiO₂ ▪ SiNx ▪ Polyimide ▪ Epoxy 	<ul style="list-style-type: none"> ▪ Benzocyclobutene ▪ Epoxy 	<ul style="list-style-type: none"> ▪ Benzocyclobutene ▪ Epoxy

Figure 1. Schematic diagrams and photographs of implanted device platforms. The table lists the main constituent materials.

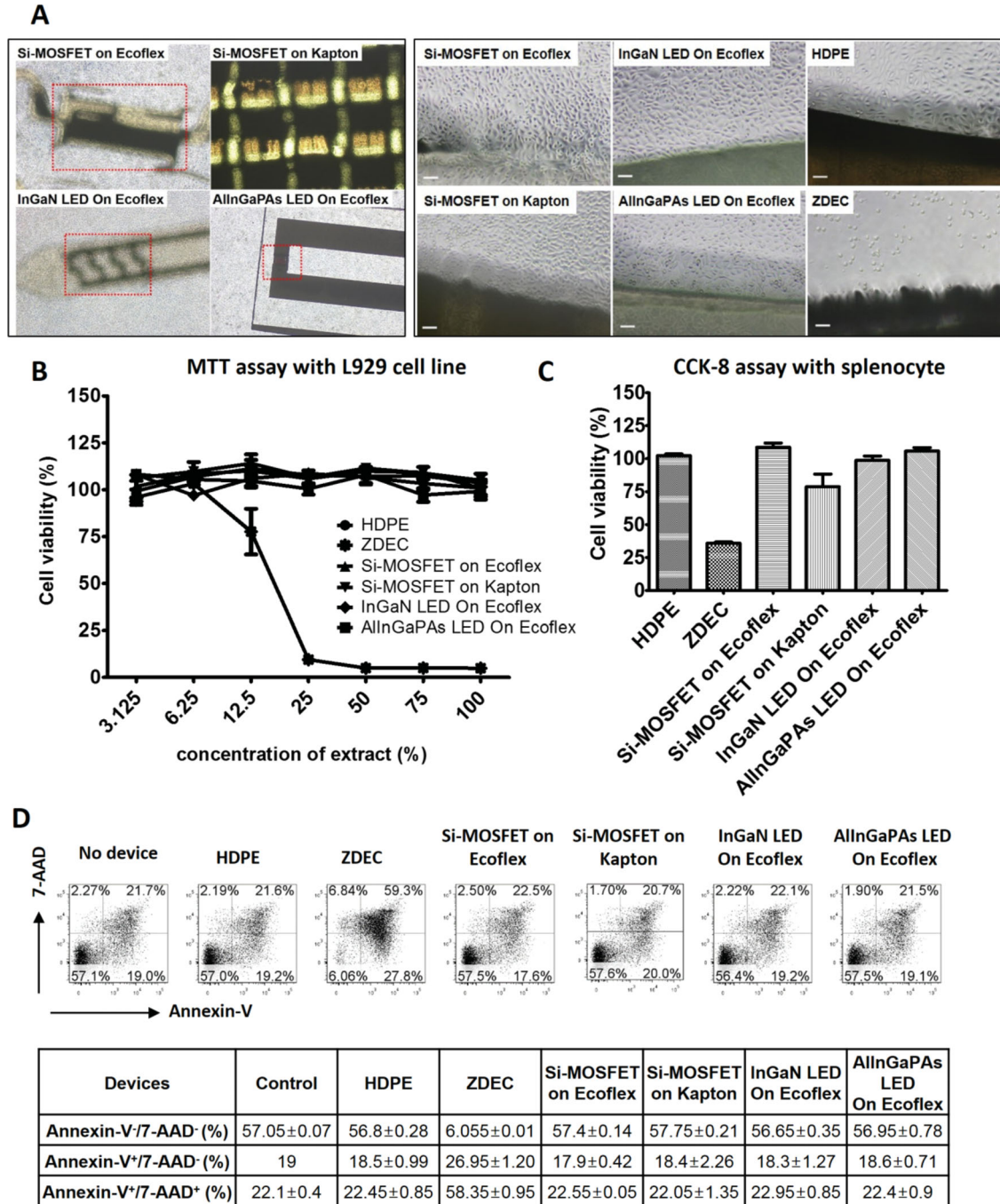


Figure 2. Direct contact cytotoxicity and apoptosis of cells exposed to flexible devices. A) Optical image of L929 fibroblasts on devices after culturing for 24 h; Left, magnification at 4× to show the larger field of cells in contact with each device. Right: magnification 100×, scale bar = 100 μm. B) Percent cell viability of L929 fibroblasts exposed to device extracts as determined by MTT assay. C) Percent cell viability of splenocytes exposed to devices for 24 h as determined by CCK-8 assay. D) Estimation of apoptotic populations in splenocytes after exposure to indicated devices for 24 h as determined by Annexin V and 7-AAD staining using flow cytometry. Results correspond to the average of triplicates and represent three independent experiments.

To determine contact cytotoxicity, each device was placed on L929 cell monolayers in a 24-well plate. We visualized the cells under a microscope and observed the morphology of cells in contact with each of the device classes. In all cases, no signs of cellular lysis, intracellular granulation, or morphological changes were observed, similar to that of HDPE (Figure 2A).

On the other hand, most cells in contact with PU-ZDEC detached from the culture dish, consistent with morphologic evidence of cell death (Figure 2A). To examine leachable cytotoxicity, we extracted each device for 24 h at 37 °C and applied the extracts to L929 cells for 24 h (minimum essential medium, MEM, extraction assay). As with the direct contact

tests, the numbers of viable cells in contact with extracts of all tested devices were comparable to those of HDPE while considerably fewer viable cells were observed in the group exposed to PU-ZDEC. To quantify the fraction of viable cells, the (3-(4,5-dimethylthiazol-2-yl)-2,5-diphenyl-2H-tetrazolium bromide (MTT) assay, which evaluates cellular mitochondrial activity and is representative of cell growth, was performed. As shown in Figure 2B, little or no cytotoxicity was detected in the sample groups exposed to extracts from various devices, even at extract concentrations of up to 100%. In contrast, the viability of cells exposed to PU-ZDEC began to decline at extract concentrations of more than $\approx 3\%$ and fell to almost 0% survival when exposed to greater than 25% extract (Figure 2B). Additional cell lines that come into contact with the device (keratinocytes, fibroblasts, and embryonic fibroblasts) were also tested for toxicity using the MTT assay; no toxicity was detected.

To assess the cytotoxicity of extracts on immune cells harvested from whole spleen, we used the Cell Counting Kit-8 (CCK-8) assay.^[32] The MTT assay cannot be used for immune cells because they are non-adherent.^[33] As can be seen in Figure 2C, direct contact of whole splenocytes to device extracts showed virtually no adverse effects on cell viability as compared with HDPE. In contrast, significantly lower viability was observed in cells exposed to PU-ZDEC. To further assess processes of cell death triggered by sample extracts in splenocytes, the extent of apoptosis was analyzed by evaluating expression of Annexin V^[34] and 7AAD.^[35] The percentages of live (Annexin V-7AAD-), early apoptotic (Annexin V+7AAD-) and late apoptotic (Annexin V+7AAD+) cells exposed to each device were comparable to those of the negative control, HDPE (Figure 2D). As expected, most cells were necrotic or undergoing apoptosis when exposed to PU-ZDEC (Figure 2D).

2.2. In Vivo Cytotoxicity and Histology Studies

To determine long-term cytotoxicity and biocompatibility, we adopted an animal model using BALB/c mice and subcutaneous implantation. A 2-cm sagittal skin incision was made on the upper back of the mouse, to create subcutaneous pockets on both the left and right sides. A piece of HDPE, as a control, was implanted on the left side; a device was implanted on the right side of the mouse. The wound was closed with metallic clips (Figure 3A). Mice were returned to the specific pathogen free (SPF) facility and monitored for the following four weeks. All device-implanted mice behaved normally and their body weight increased in parallel to that of the sham-operated controls (Figure 3B), indicating that implanted devices did not cause acute inflammatory reactions. The negative control HDPE and all devices were found to adhere to the dermis of the skin, thus preventing unwanted dislodgement from the implanted site (Figure 4A). Immunohistochemical staining of tissues surrounding each device demonstrated that the normal dermal/epidermal structure was maintained in all cases. (Figure 4B). The numbers of polymorphonuclear cells (PMC) present in the implanted sites of all four sample devices were comparable to those of the corresponding control sample, HDPE (Figure 4C). Furthermore, the degree of fibrosis, measured by the thicknesses of collagen fibers, was also no different between the

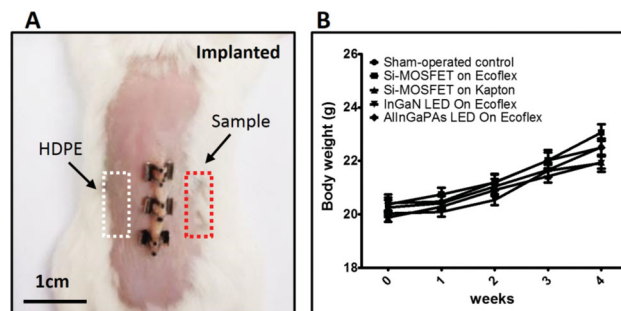


Figure 3. Subcutaneous implantation of device platforms and control samples into mice. A) Dorsal view of athymic female mouse showing subcutaneous implantation of the devices ($n = 7$). B) Average animal body weight post subcutaneous implantation of devices up to four weeks post-implantation ($n = 7$).

samples and the negative control groups (Figure 4C). The numbers of lymphocytes and capillaries formed (neovascularization) near the implanted sites were also negligible, without any statistically significant differences between the devices and the HDPE in each mouse (Table 1).

2.3. In Vivo Immunological Responses

We next investigated whether device implantation causes systemic immune reactions over a four week period following implantation. To this end, we performed immunoprofiling of lymphocytes from the blood of both sham-operated and device-implanted mice at the time of harvest. As seen in Figure 5, the percentages of CD4+ T cells, B cells, NK cells, and neutrophils in all device-implanted and sham-operated mice were found not to be significantly altered (Figure 5A,C,D,E). Interestingly, the percentages of CD8+ T cells in mice implanted with InGaN and AlInGaPAs LEDs were slightly higher than sham-operated control mice (Figure 5B). However, these changes in CD8+ T cells were not detected in the spleen (Figure S1, Supporting Information). Moreover, no substantial differences in the various lymphocyte subsets were observed between the sham-operated and device-implanted mice in the spleen (Figure S1, Supporting Information). Consistent with the immune profiling data, no significant changes in the concentration of pro-inflammatory cytokines were detected in peripheral blood samples at four weeks post-implantation as determined by cytokine measurement assays (Figure 6). Expression of representative pro-inflammatory cytokines (IL-6, MCP-1, IFN- γ , TNF- α , and IL-12p70) and anti-inflammatory cytokine IL-10^[36] was comparable in all sham-operated and device-implanted mice (Figure 6). Taken together, these data suggest that all four classes of devices are safe and non-immunogenic and have potential for use as long-term implantable components for in vivo diagnostic and therapeutic purposes.

3. Discussion

Analyses of tissue and immunological factors associated with biocompatibility in a diverse, representative set of flexible/

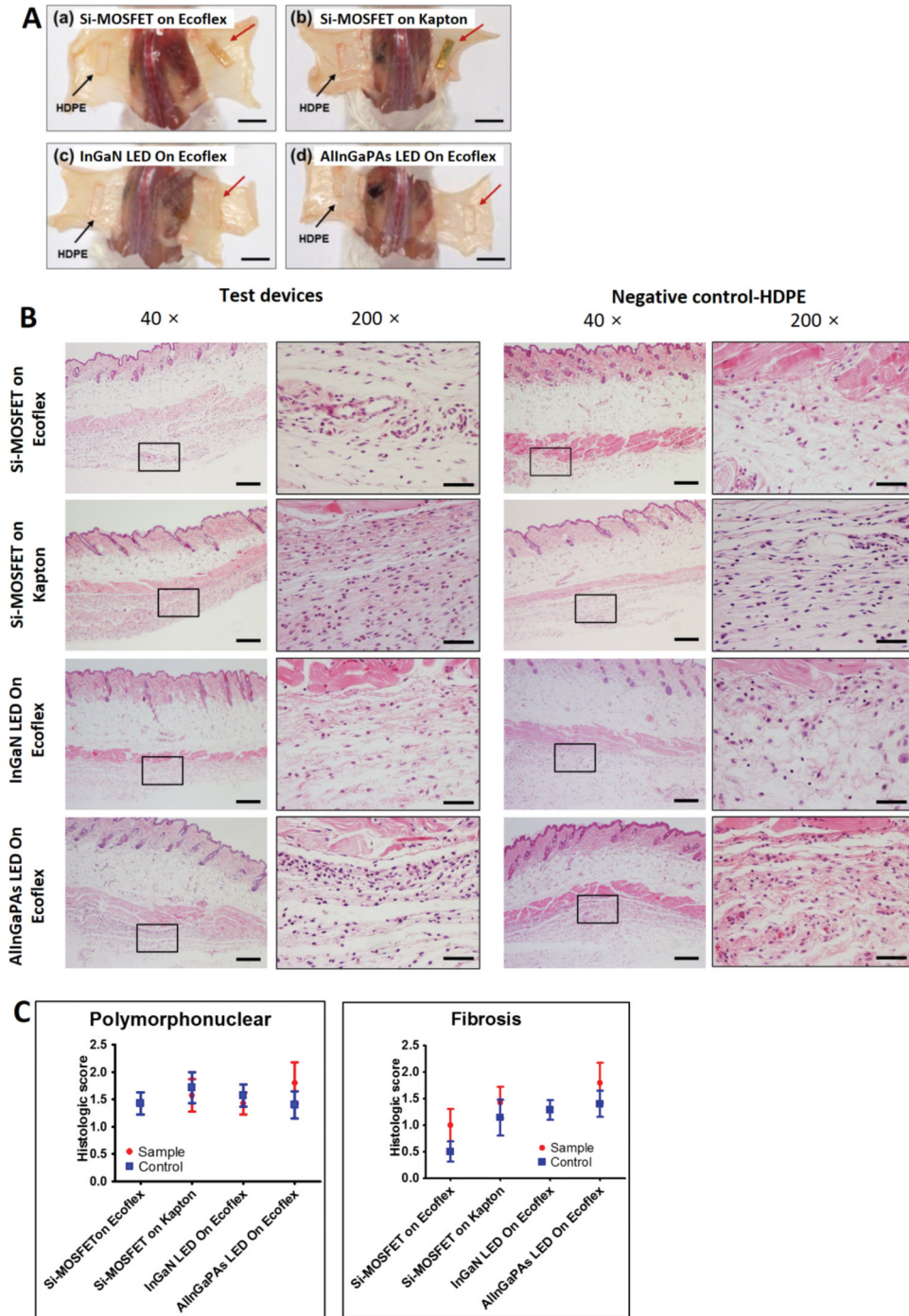


Figure 4. Histology at four weeks of post-implantation of device platforms in mice. A) Photographs of implanted device and control HDPE samples. B) Immunohistochemistry of tissues surrounding implanted devices. Individual tissue sections surrounding implanted device were subjected to H&E staining and photographed. Left panels: magnification 40 \times , scale bar = 200 μ m. Right panels: magnification 200 \times (the box shown in B is the area magnified to 200 \times), scale bar = 50 μ m. C) Histological scores of tissue adjacent to subcutaneously implanted device, as indicated. Histological scores of polymorphonuclear cell (neutrophil) and fibrosis were determined for skin biopsies excised at four weeks post-implantation.

stretchable electronic and optoelectronic platforms yield a baseline of information relevant to envisioned applications in acute implants. The investigations reveal not only local tissue factors but also immunologic parameters associated with both acute

and chronic reaction. In all cases, direct cytotoxicity and leachable cytotoxicity using an index fibroblast cell line and murine splenocytes indicated no measurable differences in percent cell viability from negative controls while exposures to positive

Table 1. Quantitative analysis of biocompatibility at four weeks of post-implantation. Tissue sections adjacent to implanted devices were stained by H&E and scored. PMC (polymorphonuclear cellular) and lymphocytic infiltration were scored according to number of cells/phf. The recruitment and activation of polymorphonuclear neutrophils (PMC), along with lymphocytes, reflect a primary reaction to foreign bodies and a measure of inflammation. Fibrosis and neovascularization were scored as described.

Implant		PMC ^{a)}	Lymphocyte ^{b)}	Fibrosis ^{c)}	Neovascularization ^{d)}
Sham-operation control		1.33 ± 0.5	–	1	–
Si-MOSFET on Ecoflex	HDPE	1.43 ± 0.53	1	0.64 ± 0.22	1
	sample	1.43 ± 0.53	1	1.00 ± 0.55	1
Si-MOSFET on Kapton	HDPE	1.71 ± 0.76	1	1.14 ± 0.55	1
	sample	1.57 ± 0.79	1	1.43 ± 0.79	1
InGaN LED On Ecoflex	HDPE	1.57 ± 0.53	–	1.29 ± 0.49	–
	sample	1.43 ± 0.53	–	1.29 ± 0.49	1.5 ± 0.71
AlInGaPAs LED On Ecoflex	HDPE	1.40 ± 0.55	–	1.40 ± 0.55	2 ± 1.41
	sample	1.80 ± 0.84	–	1.80 ± 0.84	1.2 ± 0.45

^{a)}Polymorphonuclear cells: 1–5/phf* (1), 5–10/phf(2), >10/phf (3); ^{b)}Lymphocyte: 1–5/phf (1), 5–10/phf(2), >10/phf (3); ^{c)}Fibrosis: Narrow band (1), Moderately thick band (2), Thick band (3); ^{d)}Neovascularization: 1) Minimal capillary proliferation, 2) Groups of 4–7 capillaries, 3) Broad band of capillaries; * phf = per high powered (400x) field.

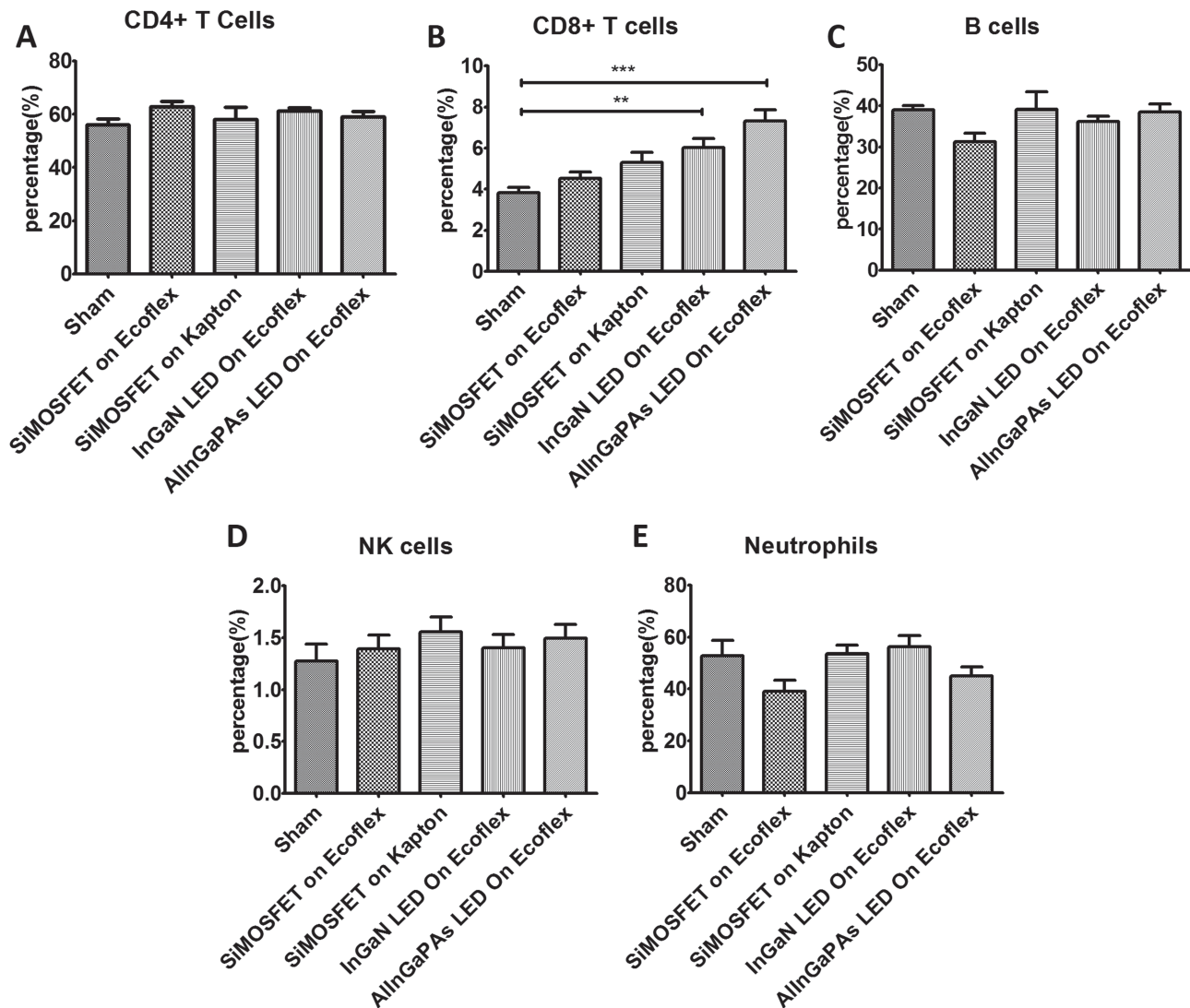


Figure 5. Immunoprofiling of cell populations in peripheral blood at 4 weeks of post-implantation of device platforms in mice. The individual immune subsets (CD4, CD8, B cell, NK cell, and neutrophils) are presented as% of total PBMCs in the peripheral blood, as measured by flow cytometry described under Materials and Methods. The averages of a total of seven samples for each data point are shown (mean ± S.E.M.). A) CD4+ T cells, B) CD8+ T cells, C) B cells, D) NK cells, and E) Neutrophils.

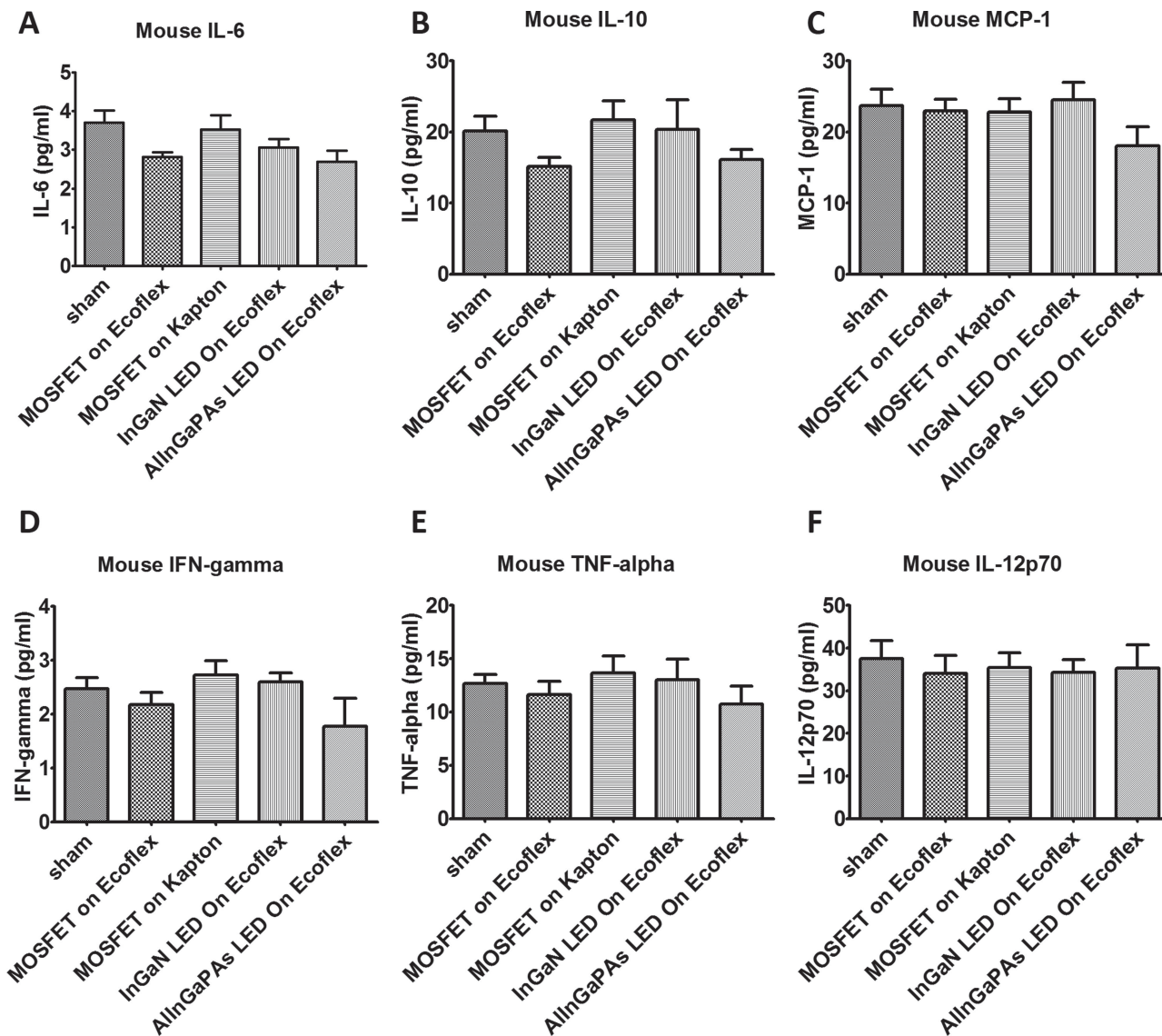


Figure 6. Immune cytokine profile measured in the peripheral blood at 4 weeks of post-implantation of device platforms in mice. The concentration of indicated cytokines in peripheral blood 4 weeks post-implantation ($n = 7$, mean \pm SEM). A) Mouse IL-6, B) IL-10, C) MCP-1, D) IFN-gamma, E) TNF alpha, and F) IL-12p70.

control samples were consistently cytotoxic. In vivo studies indicate no significant alterations in the immune cytokine panel composed of cytokines and chemokines associated with inflammation. Serum levels of IL-6 and TNF-alpha, responsible for induction of the hepatic response to inflammation and release of acute phase reactants,^[37] the Th1-type pro-inflammatory cytokines, IFN-gamma, and IL-12, and the chemokine, MCP-1, a chemoattractant for monocytes, T cells, and dendritic cells to sites of inflammation^[38,39] are comparable between experimental and sham-operated animals. Similarly, histologic grading of local tissue reaction to the implanted devices provides no evidence of increased mononuclear cellular infiltration or fibrosis after four weeks.

With the exception of an increase in the CD8 population among animals receiving AlInGaPAs LED devices on silicone,

there were no systemic changes in immune cell profile (CD4, NK, B cells and neutrophils). The presence of As in the device raises concerns about toxicity upon exposure by implantation. Indeed, a single dose of 10, 30, or 100 mg kg⁻¹ of GaAs particles, soluble under physiologically relevant in vitro conditions, was shown to produce dose-related increases in blood arsenic levels, although gallium in the blood was not detected^[40] (Among the three As containing semiconductor materials, a comparative toxicity study by Tanaka revealed that InAs was the most toxic material to the lung, followed by GaAs and AlGaAs when introduced intratracheally.)^[39] However, our data demonstrate no visible cytotoxicity of AlInGaPAs LEDs in mice when implanted subcutaneously, indicating that As in the implanted device was securely encapsulated. Interestingly, Ga is known to have an immunomodulatory effect on T cells, but has largely

been shown to be immunosuppressive.^[37,38] Although the increase in circulating CD8 T cells cannot be fully explained by exposure to Ga, certain reports suggest that AlInGaPAs can enhance antigen processing^[37] and expression of costimulatory molecules on macrophages^[39] leading, to a limited increase in T-cell proliferation. Nevertheless, the local immunosuppressive property of Ga^[37,38] may be an intrinsic benefit to the use of devices that incorporate AlInGaPAs or InGaN by its ability to limit local inflammation and mitigate immune reactivity to other device components.

Finally, it is worthwhile to note the versatility of the selected four device families. The flexible FETs on polyimide were demonstrated as basic building blocks of switches and amplifiers for wide-ranging systems, including those for electrophysiological mapping.^[6,16] These devices as well as the FETs on stretchable substrate use advanced designs, compatible with standard semiconductor process technology.^[41,42] The performance and the stability of operation are excellent, made possible by the use of high-quality thermal oxide for gate insulator and passivation.^[41,42] The AlInGaPAs LEDs emit red light and can be used for tissue imaging, spectroscopy and others; previous experiments demonstrated waterproof optical proximity sensors for advanced surgical devices.^[17] The InGaN LEDs emit blue light, and have been used in areas such as optogenetics, where the behavior of mice can be controlled by wirelessly powered cellular-scale InGaN LEDs implanted in the mice's brain.^[43] Without the limitations imposed by host immunogenicity and adverse reactivity to these components, it will be possible to transform existing short-term devices such as those already designed for high-resolution electrocorticography, multifunctional "epidermal" electronics mapping of cardiac electrophysiology into long-term implantable devices as well as entertain new applications for long-term and possibly life-long situ monitoring.

4. Conclusion

A systematic evaluation of the biocompatibility and toxicity of fully integrated, flexible/stretchable electronic and optoelectronic sub-systems presented in this report provides promising evidence for their suitability for use as long-term implantable devices. The combination of materials and process methods used to generate the devices examined in these studies are identical to those used in prior device works and represent prototypic models for future production and development. These results establish a biocompatibility profile for such implantable devices and provide reference parameters by which future designs can be compared for safety and toxicity. Establishing long-term biocompatibility now affords the opportunity to design permanent or semi-permanent devices that incorporate self-contained power and communication systems without a requirement for direct physical access.

5. Experimental Section

Control Samples: High-density polyethylene and polyurethane containing 0.1% PU-ZDEC (Hatano Research Institute, Japan)

served as negative and positive controls, respectively. The negative control is known to be inert to cells and living animals;^[44] the positive control causes cytotoxicity and inflammatory reactions upon implantation.^[44]

Substrate Materials: The substrates represent the largest area of contact between the device platforms and the target tissues. Materials for flexible devices included polyimide (PI; Kapton, DuPont) and polyethylene terephthalate (PET). Polyimide possesses chemical resistance and stability at relatively high processing temperatures; it is also well established for use in flexible neural interface devices that exploit passive arrays of electrode contacts.^[24] The biocompatibility of PI has been assessed as favorable for long-term implantation in electrode applications.^[45] PET is transparent, making it useful as a flexible substrate for implantable LEDs and photodetectors.^[17] The use of PET is widely approved in medical implants including vascular grafts, tendon and ligament substitutes, bulk space fillers, replacement joints, and spin instrumentation.^[46] For stretchable substrates, polysiloxane (silicone), which is routinely found in cosmetic and therapeutic implants,^[46] was used. Poly(dimethylsiloxane) (PDMS), the most popular material among this family, is nontoxic and biocompatible.^[47–49] In stretchable electronics, a room temperature vulcanizing (RTV) silicone material, sold under the trade name Ecoflex (Smooth-On Inc.),^[18,50] was used due to its low modulus and high elongation at break. The cytotoxicity and biocompatibility of this material are not, however, well established.

Materials, Architectures, and Processes for Flexible/Stretchable Device Components: Four types of flexible/stretchable device platforms (silicon FETs on Kapton, silicon FETs on Ecoflex, InGaN LEDs on Ecoflex, and AlInGaAsP LEDs on Ecoflex) were fabricated for in vitro cytotoxicity tests and in vivo biocompatibility assays (Figure 1, Supporting Information). In contrast to flexible transistors and LEDs based on organic materials, these platforms offer levels of performance and reliability in operation that approach those of conventional, wafer-based technologies. Flexible and stretchable mechanics are achieved by use of ultrathin device geometries, in overall layouts that minimize strains associated with bending or stretching of the supporting substrates.^[51] The fabrication began with formation of thin membranes of inorganic semiconductor materials and certain of the metal and dielectric layers. Printing-like techniques enabled integration onto a substrate of interest, where the fabrication is completed to yield systems with desired functionality. Detailed descriptions of fabrication procedures for silicon FETs on Kapton, InGaN LEDs on Ecoflex, and AlInGaPAs LEDs on Ecoflex can be found in references,^[6,52] and,^[53] respectively. A step-by-step example for the case of silicon FETs on Ecoflex appears in the Supporting Information. For consistency, all device platforms studied here have overall lateral dimensions of 10 mm × 3 mm. Material level toxicity and biocompatibility data exist for many of the constituent materials in these platforms. For example, silicon^[54] and GaN^[55] are known to be non-toxic and biocompatible, whereas GaAs exhibits certain levels of toxicity.^[56] The passive components, ranging from the polymers (polyimide,^[57] benzocyclobutene (BCB),^[58] and epoxy (SU-8; Microchem)^[54] to the inorganics (SiO₂ and SiN_x^[54]) are non-toxic and biocompatible. According to studies on the biocompatibility of dental implanting metals, Au, Pt, Pd, In, and Ti are reported to be non-toxic and biocompatible, whereas Cr and Ni are calcinogenic.^[59,60] While we did not perform a rigorous evaluation of the devices with and without full encapsulation, it is highly likely that some fraction of the devices studied were not fully encapsulated, due to point defects. As a result, the findings reported here are likely valid both for fully as well as partially encapsulated devices.

Cell Cultures: Mouse fibroblasts from a clone of strain L (NCTC clone 929, KCLB-10001; KCLB, Korea) were cultured in supplemented Eagle's minimum essential medium (MEM, 10% fetal bovine serum, 4 × 10⁻³ mL⁻¹ glutamate, 100 units mL⁻¹ of penicillin and 100 Ig mL⁻¹ of streptomycin) and incubated at 37 ± 2 °C in a humidified atmosphere with 5% CO₂. Spleens from C57BL/6 mice were homogenized using a 70 μm cell strainer (BD Biosciences, USA) to produce single cells. Splenocytes were cultured in RPMI-1640 (Welgene, Deagu, Korea) supplemented with 5% fetal bovine serum, antibiotics (penicillin

100 U mL⁻¹, streptomycin 100 µg mL⁻¹), 1× NEAA (Lonza Walkersville Inc., MD, USA), 1 × 10⁻² M HEPES Buffer, 1 × 10⁻³ M sodium pyruvate (Cellgro, VA, USA), 55 M 2-ME (Gibco, CA, USA), 1 µg mL⁻¹ anti-CD3 (clone 2C11), 1 µg mL⁻¹ anti-CD28 (clone 37.51, eBioscience, CA, USA) and 500 U mL⁻¹ interleukin (IL) - 2 (NIH, USA).

Direct Contact Tests: Mouse fibroblasts from a clone of strain L (NCTC clone 929, KCLB-10001; KCLB, Korea), seeding density 2 × 10⁵ per well were precultured for 24 h in Eagle's MEM supplemented with 10% fetal bovine serum in 24-well plates and exposed for 24 h to the samples placed in the center of each well, covering 1/10 of the cell layer surface. The morphological changes indicating cytotoxicity and cell growth characteristics were recorded as photographs using an inverted microscope (CKX41, Olympus, Tokyo, Japan).

MEM Extraction and MTT tests: Toxicity due to components of the device that solubilize or leach into solution are evaluated under "extracting" conditions. These extracting conditions attempt to simulate clinical use conditions. In general, exposure to isotonic, sterilized media (MEM) for 24 h at body temperature (37 °C) will allow for extraction of leachable material from the device into solution. Indicator cells are then exposed to the soluble extract and toxicity determined using the a viability (MTT) assay. Extracts were prepared, at a ratio of 6 cm² of the sample surface area to 1 mL of extraction vehicle (culture media), by extracting samples for 24 h at 37 °C in borosilicate glass tubes. L-929 mouse fibroblasts (seeding density at 1 × 10⁴ per well) were precultured for 24 h in 96-well plates and exposed in quadruplicates to the tested gel extracts (undiluted, 75%, 50%, 25%, 12.5%, 6.25%, and 3.125% diluted in MEM) for 24 h. For cytotoxicity testing, the extracts were sterile filtered using a 0.22-µm syringe filter. The pore size is big enough to allow passage of toxic substances. Autoclaving and ethylene oxide treatment were excluded as sterilizing methods due to possible alterations in device materials from high autoclave temperatures and infeasibility of gas treatment on liquid materials, respectively. The cells were incubated for 2 h with 1 mg mL⁻¹ MTT solutions (3-(4,5-dimethylthiazol-2-yl)-2,5-diphenyl-2H-tetrazolium bromide, Sigma, USA) under cell culture conditions. 100 µL of DMSO was then added to each well after removing supernatant medium to dissolve the internalized purple formazan crystals. Absorbance was determined and recorded using a microplate spectrophotometer (iMark, Bio-RAD) at wavelengths of 570 nm and 650 nm. The results were expressed as a percentage of the absorbance of the control.

Cell Count Kit-8 (CCK-8) Tests: The viability of splenocytes in contact with sample materials and devices was measured by Cell Counting Kit-8 (CCK-8; Dojindo Laboratories, Kumamoto, Japan) according to the manufacturer's instruction. Briefly, splenocytes were incubated with indicated samples on 24-well plates for 24 h before addition of 10% of CCK-8 solution. Cells were then incubated for an additional 2 h at 37 °C to form water-dissolvable formazan. 50 µL of this formazan solution was collected from each sample and added to one well of a 96-well plate. Three parallel replicates were prepared. The absorbance at 450 nm was determined using a microplate spectrophotometer (iMark, Bio-RAD).

Apoptosis Assays: After incubation with the samples, the cells were stained according to the general Annexin V staining procedure by BD Biosciences (Annexin V-FITC Apoptosis detection kit 1, BD Biosciences, San Diego, US). Splenocytes were then analyzed for their expression of Annexin V and 7-Amino-Actinomycin D (7-AAD) to determine the number of viable cells: Annexin V and 7AAD negative (Annexin V⁻/7AAD⁻); cells undergoing apoptosis, Annexin V positive and 7AAD negative (Annexin V⁺/7AAD⁻); and dead cells or cells that were in latest stage of apoptosis, Annexin and 7-AAD positive (Annexin V⁺/7AAD⁺).

In Vivo Tissue Biocompatibility Tests: Sterile implant samples, each approximately 3 mm × 10 mm, were prepared aseptically. USP negative controls (HDPE) of the same dimensions were sterilized by EO gas. Mice were implanted with the two samples, one test and one negative, for periods of four weeks, and were euthanized prior to excising muscle tissue and examining the implant site macroscopically. The inserted devices initially adhered to the subcutaneous layers (hypodermis) due to adequate adhesion to the skin layer based on van der Waals

interactions.^[18] A thin transparent layer of fibroblasts was found growing over the devices, thus stabilizing the inserted device in their place. A microscopic evaluation was conducted to further define any tissue response. Implant sites were examined microscopically for signs of inflammation such as the presence of PMC, lymphocytes, plasma cells, macrophages, giant cells, and gross necrosis. They were also examined for fibroplasia, fibrosis, and fatty infiltrates

Surgical Procedures: Four devices were sterilized with ethylene oxide gas. All animal experiments were approved by Institutional Animal Care and Use Committees of Korea University and performed in accordance with national and institutional guidelines. The animals were anesthetized with a mixture of 30 mg kg⁻¹ zolazepam hydroxide (Zoletil 50; Virbac, Sao Paulo, Brazil) and 10 mg kg⁻¹ xylazine hydroxide (Rumpun; Bayer, Shawnee Mission, KS) via intraperitoneal injection. After the induction of anesthesia, the hair on the back was shaved around the implantation site and the skin was sterilized by brushing with a 70% ethanol solution. An incision was made with scissors on side of the shaved skin of the back, and a specimen was inserted subcutaneously. Control animals were treated by a sham operation with no implantation. After the operation, euthanized mice were clipped and sterilized with serial washes in povidone iodine and ethanol solutions. During the experimental period, body weight and health conditions were monitored. All procedures were approved by Korea University Institutional Animal Care & Use Committee (KUIACUC-2013-93).

Cytometric Bead Arrays (CBA) for Measuring Cytokines: Peripheral blood was collected from mice and serum was separated by centrifugation at 5000 rpm for 10 min. Serum concentrations of IL-6, IL-10, MCP-1, IFN-γ, TNF, and IL-12p70 were measured using a CBA Mouse Inflammation Kit (BD Biosciences, San Diego, CA), according to the manufacturer's instructions, with some modification. Briefly, 15 µL of capture bead mixture was incubated with 40 µL of each recombinant standard or sample and 15 µL PE-conjugated detection antibody for 2 h at room temperature. The sample was then washed and analyzed by flow cytometry per the manufacturer's instructions.

Flow Cytometry Analyses: Anti-mouse CD4 (RM4-4), Ly6G (RB6-8C5), CD3 (145-2C11), CD19 (1D3), CD49b (Dx5), CD8 (53-6.7), CD11b (M1/70) monoclonal antibodies (mAbs) conjugated with fluorescein isothiocyanate (FITC), phycoerythrin (PE), phycoerythrin-cyanine dye (PE-Cy7), peridinin chlorophyll protein complex with cyanin-5.5 (PerCP-Cy 5.5), allophycocyanin (APC), allophycocyanin-cyanine dye (APC-Cy7), Alexa Fluor 488 were purchased from eBioscience (San Diego, CA, USA). Isolated cells were resuspended in 100 µL of FACS buffer (PBS containing 2% FBS and 0.02% sodium azide) and incubated with anti-CD16/CD32 mAb (2.4G2, Fc block) to block FcR1/II receptors. Cells were then incubated for 20 min at 4 °C. Flow cytometry was performed with a FACS Canto II (BD Bioscience, San Diego, CA, USA) and the data analyzed with FlowJo software (ThreeStar, USA). Fifty thousand lymphocyte populations gated by forward scatter (FCS)/side scatter (SSC) were analyzed.

Histological Studies: Mice were euthanized via CO₂ asphyxiation and the implanted samples and surrounding tissue were excised. The tissues were then fixed in 10% formalin, embedded in paraffin, cut into 4 µm sections, and stained using hematoxylin and eosin (H&E) for histological analysis. Each sample was analyzed in blinded fashion by a board certified pathologist, Dr. Chan-Shik Park at the University of Ulsan, Asan Hospital in Seoul.

Statistics: All data are represented as mean ± SEM of three identical experiments made in three replicates. Statistical significance was determined by one-way analysis of variance (ANOVA) followed by Dunnett's multiple comparison test. Significance was ascribed at *p* < 0.05. All analyses were conducted using the Prism software (Graph Pad Prism 5.0).

Supporting Information

Supporting Information is available from the Wiley Online Library or from the author.

Acknowledgements

G.P. and H.-J.C. contributed equally to this work. This work was supported by the Korea Foundation for International Cooperation of Science & Technology (KICOS) grant (K20703001994-12A0500-03610) and the Converging Research Center Program (2012K001404). J.A.R. is supported by a National Security Science and Engineering Faculty Fellowship. K.-M.L. is additionally supported by the National Research Foundation of Korea Grant, 013-2011-1-E00011. H.-J.C. acknowledges Dr. M. H. Lee (FDA, USA) for insightful discussions throughout the study.

Received: June 5, 2013

Revised: June 29, 2013

Published online: September 1, 2013

- [1] W. Greatbatch, C. F. Holmes, *IEEE Eng. Med. Biol.* **1991**, *10*, 38.
- [2] F. G. Zeng, S. Rebscher, W. Harrison, X. Sun, H. Feng, *IEEE Rev. Biomed. Eng.* **2008**, *1*, 115.
- [3] J. S. Perlmutter, J. W. Mink, *Annu. Rev. Neurosci.* **2006**, *29*, 229.
- [4] J. Viventi, D.-H. Kim, J. D. Moss, Y.-S. Kim, J. A. Blanco, N. Annetta, A. Hicks, J. Xiao, Y. Huang, D. J. Callans, J. A. Rogers, B. Litt, *Sci. Transl. Med.* **2010**, *2*, 24ra22.
- [5] D. H. Kim, J. Viventi, J. J. Amsden, J. Xiao, L. Vigeland, Y. S. Kim, J. A. Blanco, B. Panilaitis, E. S. Frechette, D. Contreras, D. L. Kaplan, F. G. Omenetto, Y. Huang, K. C. Hwang, M. R. Zakin, B. Litt, J. A. Rogers, *Nat. Mater.* **2010**, *9*, 511.
- [6] J. Viventi, D. H. Kim, L. Vigeland, E. S. Frechette, J. A. Blanco, Y. S. Kim, A. E. Avrin, V. R. Tiruvadi, S. W. Hwang, A. C. Vanleer, D. F. Wulsin, K. Davis, C. E. Gelber, L. Palmer, J. van der Spiegel, J. Wu, J. Xiao, Y. Huang, D. Contreras, J. A. Rogers, B. Litt, *Nat. Neurosci.* **2011**, *14*, 1599.
- [7] D. H. Kim, S. Wang, H. Keum, R. Ghaffari, Y. S. Kim, H. Tao, B. Panilaitis, M. Li, Z. Kang, F. Omenetto, Y. Huang, J. A. Rogers, *Small* **2012**, *8*, 3263.
- [8] J. H. Ahn, J. H. Je, *J. Phys. D: Appl. Phys.* **2012**, *45*, 103001.
- [9] T. Someya, Y. Kato, T. Sekitani, S. Iba, Y. Noguchi, Y. Murase, H. Kawaguchi, T. Sakurai, *Proc. Natl. Acad. Sci. U. S. A.* **2005**, *102*, 12321.
- [10] K. Huang, P. Peumans, *Proc. SPIE* **2006**, *6174*, 617412.
- [11] R. Dinyari, S.-B. Rim, K. Huang, P. B. Catrysse, P. Peumans, *Appl. Phys. Lett.* **2008**, *92*, 091114.
- [12] C. Cheng, V. K. M. Mushahwar, A. L. Elias, *IEEE Trans. Biomed. Eng.* **2013**, *60*, 1667.
- [13] S. Wagner, S. P. Lacour, J. Jones, P.-h. I. Hsu, J. C. Sturm, T. Li, Z. Suo, *Physica E* **2004**, *25*, 326.
- [14] V. Vanfleteren, M. Gonzalez, F. Bossuyt, Y.-Y. Hsu, T. Vervust, I. De Wolf, M. Jablonski, *MRS Bull.* **2012**, *37*, 254.
- [15] G. S. Jeong, D.-H. Baek, H. C. Jung, J. H. Song, J. H. Moon, S. W. Hong, I. Y. Kim, S.-H. Lee, *Nat. Commun.* **2012**, *3*, 977.
- [16] C. Pang, G.-Y. Lee, T.-i. Kim, S. M. Kim, H. N. Kim, S.-H. Ahn, K.-Y. Suh, *Nat. Mater.* **2012**, *11*, 795.
- [17] R. H. Kim, D. H. Kim, J. Xiao, B. H. Kim, S. I. Park, B. Panilaitis, R. Ghaffari, J. Yao, M. Li, Z. Liu, V. Malyarchuk, D. G. Kim, A. P. Le, R. G. Nuzzo, D. L. Kaplan, F. G. Omenetto, Y. Huang, Z. Kang, J. A. Rogers, *Nat. Mater.* **2010**, *9*, 929.
- [18] D. H. Kim, N. Lu, R. Ma, Y. S. Kim, R. H. Kim, S. Wang, J. Wu, S. M. Won, H. Tao, A. Islam, K. J. Yu, T. I. Kim, R. Chowdhury, M. Ying, L. Xu, M. Li, H. J. Chung, H. Keum, M. McCormick, P. Liu, Y. W. Zhang, F. G. Omenetto, Y. Huang, T. Coleman, J. A. Rogers, *Science* **2011**, *333*, 838.
- [19] D. H. Kim, N. Lu, R. Ghaffari, Y. S. Kim, S. P. Lee, L. Xu, J. Wu, R. H. Kim, J. Song, Z. Liu, J. Viventi, B. de Graff, B. Elolampi, M. Mansour, M. J. Slepian, S. Hwang, J. D. Moss, S. M. Won, Y. Huang, B. Litt, J. A. Rogers, *Nat. Mater.* **2011**, *10*, 316.
- [20] M. Ying, A. P. Bonifas, N. Lu, Y. Su, R. Li, H. Cheng, A. Ameen, Y. Huang, J. A. Rogers, *Nanotechnology* **2012**, *23*, 344004.
- [21] D. H. Kim, R. Ghaffari, N. Lu, S. Wang, S. P. Lee, H. Keum, R. D'Angelo, L. Klinker, Y. Su, C. Lu, Y. S. Kim, A. Ameen, Y. Li, Y. Zhang, B. de Graff, Y. Y. Hsu, Z. Liu, J. Ruskin, L. Xu, C. Lu, F. G. Omenetto, Y. Huang, M. Mansour, M. J. Slepian, J. A. Rogers, *Proc. Natl. Acad. Sci. U. S. A.* **2012**, *109*, 19910.
- [22] D. H. Kim, R. Ghaffari, N. S. Lu, S. D. Wang, S. P. Lee, H. Keum, R. D'Angelo, L. Klinker, Y. W. Su, C. F. Lu, Y. S. Kim, A. Ameen, Y. H. Li, Y. H. Zhang, B. de Graff, Y. Y. Hsu, Z. J. Liu, J. Ruskin, L. Z. Xu, C. Lu, F. G. Omenetto, Y. G. Huang, M. Mansour, M. J. Slepian, J. A. Rogers, *Proc. Natl. Acad. Sci. U. S. A.* **2012**, *109*, 19910.
- [23] S. D. Wang, M. Li, J. Wu, D. H. Kim, N. S. Lu, Y. W. Su, Z. Kang, Y. G. Huang, J. A. Rogers, *J. Appl. Mech.* **2012**, *79*, 051002.
- [24] R. V. Bellamkonda, S. B. Pai, P. Renaud, *MRS Bull.* **2012**, *37*, 557.
- [25] S. Xu, Y. Zhang, J. Cho, J. Lee, X. Huang, L. Jia, J. A. Fan, Y. Su, J. Su, H. Zhang, H. Cheng, B. Lu, C. Yu, C. Chuang, T. I. Kim, T. Song, K. Shigeta, S. Kang, C. Dagdeviren, I. Petrov, P. V. Braun, Y. Huang, U. Paik, J. A. Rogers, *Nat. Commun.* **2013**, *4*, 1543.
- [26] R. H. Kim, H. Tao, T. I. Kim, Y. Zhang, S. Kim, B. Panilaitis, M. Yang, D. H. Kim, Y. H. Jung, B. H. Kim, Y. Li, Y. Huang, F. G. Omenetto, J. A. Rogers, *Small* **2012**, *8*, 2812.
- [27] M. N. Helmus, D. F. Gibbons, D. Cebon, *Toxicol. Appl. Pharmacol.* **2008**, *36*, 70.
- [28] P. Dunne, *Polym. Testing* **2005**, *24*, 684.
- [29] T. Velten, H. H. Ruf, D. Barrow, N. Aspragathos, P. Lazarou, E. Jung, C. K. Malek, M. Richter, J. Kruckow, M. Wackerle, *IEEE Trans. Adv. Packag.* **2005**, *28*, 533.
- [30] E. Velasco-Ortega, A. Jos, A. M. Camean, J. Pato-Mourello, J. J. Segura-Egea, *Mutation Res.* **2010**, *702*, 17.
- [31] W. K. Lee, K. D. Park, D. K. Han, H. Suh, J. C. Park, Y. H. Kim, *Biomaterials* **2000**, *21*, 2323.
- [32] D. C. Niu, Y. S. Li, Z. Ma, H. Diao, J. L. Gu, H. R. Chen, W. R. Zhao, M. L. Ruan, Y. L. Zhang, J. L. Shi, *Adv. Funct. Mater.* **2010**, *20*, 773.
- [33] D. Fischer, Y. X. Li, B. Ahlemeyer, J. Krieglstein, T. Kissel, *Biomaterials* **2003**, *24*, 1121.
- [34] L. Li, J. Sun, X. R. Li, Y. Zhang, Z. X. Wang, C. R. Wang, J. W. Dai, Q. B. Wang, *Biomaterials* **2012**, *33*, 1714.
- [35] L. O. Bailey, S. Lipplatt, F. S. Biancanello, S. D. Ridder, N. R. Washburn, *Biomaterials* **2005**, *26*, 5296.
- [36] W. Ji, F. Yang, H. Seyednejad, Z. Chen, W. E. Hennink, J. M. Anderson, J. J. P. van den Beucken, J. A. Jansen, *Biomaterials* **2012**, *33*, 6604.
- [37] E. H. Huang, D. M. Gabler, M. E. Krecic, N. Gerber, R. M. Ferguson, C. G. Orosz, *Transplantation* **1994**, *58*, 1216.
- [38] L. A. Burns, A. E. Munson, *J. Pharmacol. Exp. Ther.* **1993**, *265*, 178.
- [39] R. E. Caffrey-Nolan, K. L. McCoy, *Toxicol. Appl. Pharmacol.* **1998**, *151*, 330.
- [40] D. R. Webb, I. G. Sipes, D. E. Carter, *Toxicol. Appl. Pharmacol.* **1984**, *76*, 96.
- [41] H.-J. Chung, T.-i. Kim, H.-S. Kim, S. A. Wells, S. Jo, N. Ahmed, Y. H. Jung, S. M. Won, C. A. Bower, J. A. Rogers, *Adv. Funct. Mater.* **2011**, *21*, 3029.
- [42] T.-i. Kim, Y. H. Jung, H.-J. Chung, K. J. Yu, N. Ahmed, C. J. Corcoran, J. S. Park, S. H. Jin, J. A. Rogers, *Appl. Phys. Lett.* **2013**, *102*, 182104.
- [43] T. I. Kim, J. G. McCall, Y. H. Jung, X. Huang, E. R. Siuda, Y. H. Li, J. Z. Song, Y. M. Song, H. A. Pao, R. H. Kim, C. F. Lu, S. D. Lee, I. S. Song, G. Shin, R. Al-Hasani, S. Kim, M. P. Tan, Y. G. Huang, F. G. Omenetto, J. A. Rogers, M. R. Bruchas, *Science* **2013**, *340*, 211.
- [44] E. A. E. Van Tienhoven, D. Korbee, L. Schipper, H. W. Verharen, W. H. De Jong, *J. Biomed. Mater. Res. A* **2006**, *78A*, 175.

- [45] Y. Sun, S. P. Lacour, R. A. Brooks, N. Rushton, J. Fawcett, R. E. Cameron, *J. Biomed. Mater. Res. A* **2009**, *90*, 648.
- [46] S. Ramakrishna, J. Mayer, E. Wintermantel, K. W. Leong, *Compos. Sci. Technol.* **2001**, *61*, 1189.
- [47] S. I. Ertel, B. D. Ratner, A. Kaul, M. B. Schway, T. A. Horbett, *J. Biomed. Mater. Res.* **1994**, *28*, 667.
- [48] M. C. Belanger, Y. Marois, *J. Biomed. Mater. Res.* **2001**, *58*, 467.
- [49] J. N. Lee, X. Jiang, D. Ryan, G. M. Whitesides, *Langmuir* **2004**, *20*, 11684.
- [50] M. Kubo, X. Li, C. Kim, M. Hashimoto, B. J. Wiley, D. Ham, G. M. Whitesides, *Adv. Mater.* **2010**, *22*, 2749.
- [51] D. H. Kim, N. S. Lu, Y. G. Huang, J. A. Rogers, *MRS Bull.* **2012**, *37*, 226.
- [52] T. I. Kim, Y. H. Jung, J. Z. Song, D. Kim, Y. H. Li, H. S. Kim, I. S. Song, J. J. Wierer, H. A. Pao, Y. G. Huang, J. A. Rogers, *Small* **2012**, *8*, 1643.
- [53] R. H. Kim, S. Kim, Y. M. Song, H. Jeong, T. I. Kim, J. Lee, X. L. Li, K. D. Choquette, J. A. Rogers, *Small* **2012**, *8*, 3123.
- [54] G. Kotzar, M. Freas, P. Abel, A. Fleischman, S. Roy, C. Zorman, J. M. Moran, J. Melzak, *Biomaterials* **2002**, *23*, 2737.
- [55] S. A. Jewett, M. S. Makowski, B. Andrews, M. J. Manfra, A. Ivanisevic, *Acta Biomater.* **2012**, *8*, 728.
- [56] A. Tanaka, *Toxicol. Pathol.* **2004**, *198*, 405.
- [57] C. Hassler, T. Boretius, T. Stieglitz, *J. Polym. Sci., Polym. Phys. Ed.* **2011**, *49*, 18.
- [58] B. A. Koeneman, K. K. Lee, A. Singh, J. P. He, G. B. Raupp, A. Panitch, D. G. Capco, *J. Neurosci. Methods* **2004**, *137*, 257.
- [59] J. C. Hornez, A. Lefevre, D. Joly, H. F. Hildebrand, *Biomol. Eng.* **2002**, *19*, 103.
- [60] J. C. Wataha, *J. Prosthet. Dent.* **2000**, *83*, 223.